



Exploring the Galactic neutrino flux origins using IceCube datasets

Downloaded from: <https://research.chalmers.se>, 2025-06-09 14:47 UTC

Citation for the original published paper (version of record):

Abbasi, R., Ackermann, M., Adams, J. et al (2024). Exploring the Galactic neutrino flux origins using IceCube datasets. *Proceedings of Science*, 444

N.B. When citing this work, cite the original published paper.

Exploring the Galactic neutrino flux origins using IceCube datasets

The IceCube Collaboration

(a complete list of authors can be found at the end of the proceedings)

E-mail: adesai@icecube.wisc.edu

Astrophysical neutrinos detected by the IceCube observatory can be of Galactic or extragalactic origin. The collective contribution of all the detected neutrinos allows us to measure the total diffuse neutrino Galactic and extragalactic signal. In this work, we describe a simulation package that makes use of this diffuse Galactic contribution information to simulate a population of Galactic sources distributed in a manner similar to our own galaxy. This is then compared with the sensitivities reported by different IceCube data samples to estimate the number of sources that IceCube can detect. We provide the results of the simulation that allows us to make statements about the nature of the sources contributing to the IceCube diffuse signal.

Corresponding authors: Abhishek Desai¹, Jessie Thwaites^{1*}, Justin Vandenbroucke¹

^a *Dept. of Physics and Wisconsin IceCube Particle Astrophysics Center, University of Wisconsin–Madison, Madison, WI 53706, USA*

* Presenter

38th International Cosmic Ray Conference (ICRC2023)
26 July - 3 August, 2023
Nagoya, Japan



1. Introduction

The Milky Way Galaxy is home to numerous objects and matter that can lead to the production of neutrinos observable on Earth. Recently, [1] reported the observation of neutrino emission from the Galactic plane by the IceCube Neutrino Observatory, with $> 4\sigma$ significance. A confirmation of the exact nature of the sources producing these neutrinos was not found. However, speculations exist about these neutrinos originating from sources like pulsar wind nebula (PWN) or supernova remnants (SNR) or due to cosmic ray interactions (see, for example, [2–4]). Fortunately, because of the kiloparsec scale distances of sources and matter distributed across the Galaxy, these speculations can be tested and commented upon (see, for example, [5, 6]). In this work, we build upon the results we reported in [6] using additional IceCube data to comment on the nature of these neutrino-producing sources and the future of Galactic neutrino searches using IceCube.

The IceCube neutrino observatory classifies detected neutrino events into track-like or cascade-like depending on the observed event signature [7]. Track-like events have better angular resolution due to them being produced by long-lived muons that travel several kilometers in the ice. On the other hand, cascade events are short-lived but have better energy resolution. Different IceCube data samples are created using events of one of these types, along with improved reconstructions using methods like cascades with neural network [1] or track events with boosted decision tree [8]. There also exist combined samples like [9], which include both track and cascade events. All these datasets have different effective areas along with different energy and angular resolution, giving them different sensitivities and discovery potentials required to make a detection. In this work, we use the sensitivity and discovery potential curves of 4 different IceCube datasets, namely: 10-year Point Source Tracks ("PST" from this point; see also [10]), DNN Cascades ("DNN" from this point; see also [1]), Enhanced Starting Tracks Event Selection ("ESTES" from this point; see also [8, 11]) and a combined event selection made up of ESTES tracks, DNN cascades, and Northern tracks ("Combined sample" from this point; see also [9]). Note that the PS Tracks dataset used here is one reported in [10] and cannot be directly compared with the Northern tracks dataset in the combined sample by [9].

2. Neutrinos from the Galactic center

Following the procedure shown in [6], we first estimate simply the number of sources required to make up the observed neutrino emission, provided that all the sources are concentrated at the Galactic center. The observed neutrino emission is taken from the best-fit flux reported by [1] for the KRA_{γ}^{50} template. This is because the reported signal using the KRA_{γ}^{50} template [12] is more prominent at the center of the Galaxy. The best-fit flux for the KRA_{γ}^{50} template at 100 TeV is given by $\sim 1.5 \times 10^{-15} \text{ TeV}^{-1} \text{ cm}^{-2} \text{ s}^{-1}$ (Fig. 5 of [1]). For each of the tested IceCube datasets, we use the 90% sensitivity and the 5σ discovery potential curves (as reported by [9]) to determine the neutrino flux of sources making up the background assuming all sources have equal flux (as all sources are at the center the luminosities are also equal). "Flux" here denotes the differential neutrino number flux in units of $\text{TeV}^{-1} \text{ cm}^{-2} \text{ s}^{-1}$ at 100 TeV. As all the sources contribute to the total galactic neutrino flux equally, the number of sources making up the signal is derived by taking the ratio of the total flux and the per-source flux contribution.

Sample Tested	$E^{-2.0}$ Flux at $\sim 28^\circ$	N_{src} ($\gamma = -2.0$)
DNN sensitivity	1.07e-16	14
DNN 5σ DP	4.68e-16	3
PST sensitivity	2.25e-16	7
PST 5σ DP	7.97e-16	2
ESTES sensitivity	4.90e-16	3
ESTES 5σ DP	1.41e-15	1
Combined sensitivity	8.54e-17	18
Combined 5σ DP	4.08e-16	4

Table 1: Assuming that all point sources making up the observed Galactic neutrino signal are concentrated at the center, we show for each dataset the per source flux and the number of sources (N_{src}). The flux spectrum (dN/dE) is taken to be a power law with an index of 2.0. Note that as no detected Galactic neutrino sources exist, the flux estimates are taken from the sensitivity curve and treated as upper limits, while the number of sources contributing to the signal should be treated as lower limits.

When compared directly to the results presented in [6], this work includes more information in the form of the ESTES and Combined samples, along with 5σ discovery potential curve (as opposed to the 4σ discovery potential) for the DNN sample (see [9] for more details). Note that in the event that these sources are detected, they will all be clustered at the center leading to source confusion.

3. Simulating neutrino sources

We now simulate the neutrino sources in the Galaxy and compare them to sensitivity and discovery potential curves. Following the procedure described in [6], we use the "*Simulation of the Neutrino and Gamma-ray Galactic Yield*" (S*NuGGY*¹) package. In this work, to simulate source positions, we make use of a modified exponential spatial distribution given by

$$\rho(R, z) = \rho_0 \left(\frac{R}{R_\odot} \right)^\alpha \exp\left(-\beta \frac{R - R_0}{R_\odot}\right) \exp\left(-\frac{|z|}{h}\right), \quad (1)$$

where R and z are the horizontal and vertical scaling lengths respectively, and $\alpha = 2$, $\beta = 3.53$, and $h = 0.181$ are parameters for the distribution given by [13, 14]. The Jacobian factor is included while estimating the source positions, causing a shift away from the Galactic center for the R values.

The neutrino fluxes are simulated using a log-normal luminosity function where the luminosity is defined as the integrated value over an energy range of 10 TeV-10 PeV, and has units of erg/s. The

¹<https://github.com/adesai90/SNuGGY>

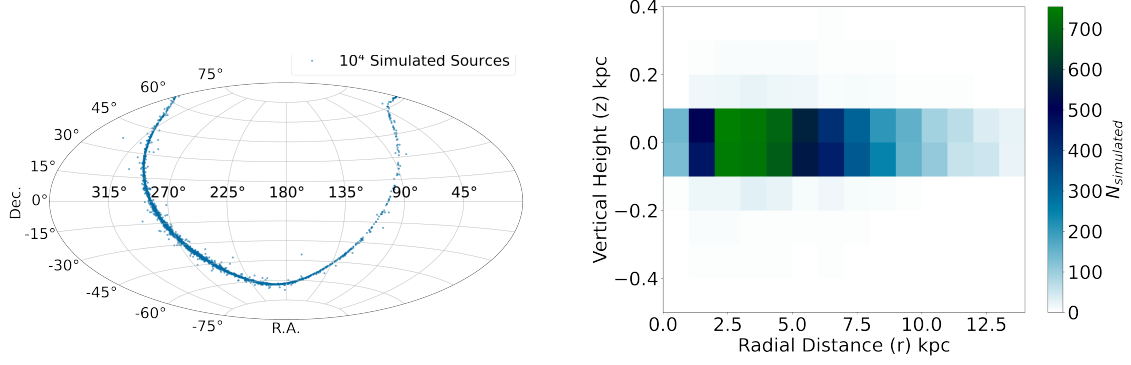


Figure 1: One simulation of 10^4 sources derived using the SNUGGY framework is shown here. The source coordinates in Galactic coordinates are shown on the left while the distribution of the scale height z and length R from equation Eq. 1 is shown on the right. Note the shift in the peak away from $R = 0$ due to the inclusion of the Jacobian factor.

luminosity distribution is given by

$$P_{LN}(L) = \frac{\log_{10}e}{\sigma_L L \sqrt{2\pi}} \exp\left(\frac{-(\log_{10}L - \log_{10}L_0)^2}{2\sigma_L^2}\right), \quad (2)$$

where the L_0 is the mean luminosity while the σ_L parameter controls the width of the distribution. The mean luminosity is calculated using

$$L_{SC} = \frac{\phi_{Galactic}}{\sum_{i=1}^N \frac{1}{4\pi d_i^2}}, \quad (3)$$

where $\phi_{Galactic}$ is the total diffuse flux and N is the number of simulated sources at a distance d_i . Note that giving a very low value of σ_L will reduce the width of the distribution and result in simulated luminosities equal to the mean luminosity (with slight deviations), mimicking a standard candle approach. For more details regarding how the source positions and neutrino fluxes are simulated, see [6].

For each simulated test case, we fix the number of simulated sources. The SNUGGY simulation ensures that the sources have a spatial distribution as shown in Fig. 1 along with a log-normal luminosity distribution. The simulated differential fluxes at 100 TeV are then used to compare with the sensitivity and discovery potential curves of the IceCube datasets. Two hypotheses are tested here: (1) All sources are close to the center of the Galaxy and (2) sources follow a PWN distribution. The latter will allow us to make assumptions about Galactic neutrino source classes as a whole, as the spatial distribution of galactic sources is similar to each other.

While a simple comparison of the simulated fluxes with the sensitivity or discovery potential fluxes is possible, actual detection of neutrinos from a source is subject to Eddington bias [16]. This bias is particularly seen for the "large number of dim sources" case, as it is seen as upward Poisson fluctuations in the number of detected neutrinos. We account for this by estimating the number of

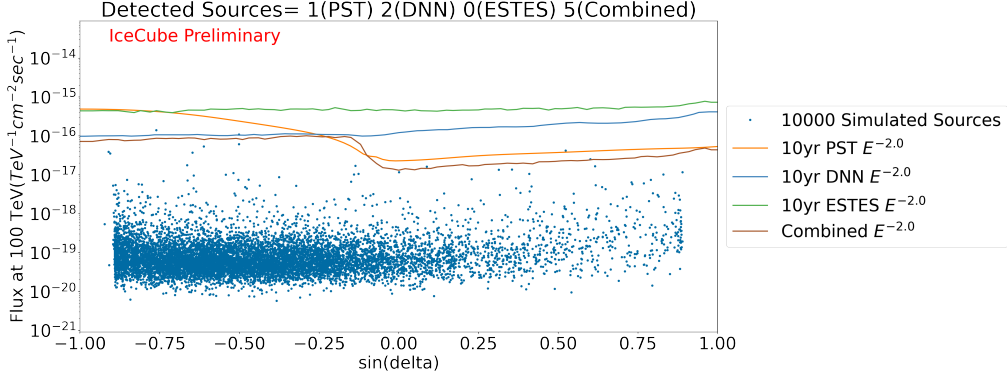


Figure 2: Comparison of simulated sources with the 90% CL sensitivity curves from the four IceCube data samples. Blue points show 10^4 simulated sources with fluxes derived using a log-normal luminosity distribution with $\sigma_L=0.01$ (similar to a SC scenario). If a simulated source flux is above the sensitivity curve, the source is counted as detected. The 10yr PST sensitivity is taken from [15], DNN from [1] and ESTES and Combined from [9].

energy-integrated neutrino events over a period of 10 years using the simulated neutrino flux and IceCube effective area and adding Poisson fluctuations to the simulated data. The effective area measurements are taken from references [10] and [9]. If the number of Poisson fluctuated neutrino events are higher than the threshold number of events derived using the sensitivity or discovery potential, the source is considered to be "detected". This calculation is repeated multiple times in the form of a Monte Carlo simulation to derive the mean number of detected sources along with a 1σ standard deviation.

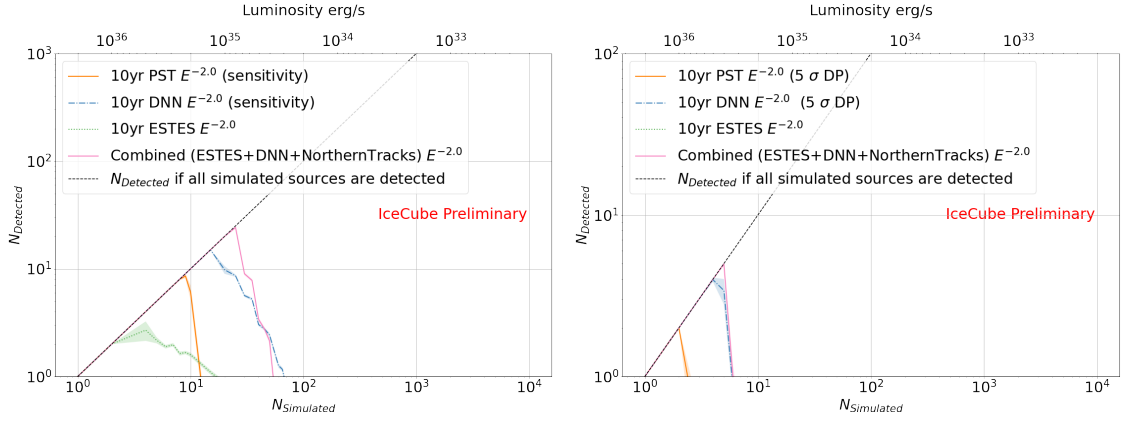


Figure 3: Special case for sources simulated at the Galactic center: The number of detected neutrino sources at the Galactic center for different sensitivity and discovery potential curves (taken from [1, 9, 15]) while using a $\sigma_L=0.01$ $\text{TeV}^{-1}\text{cm}^{-2}\text{s}^{-1}$. The left plot makes use of sensitivity curves, while the right plot makes use of discovery potential curves. The shaded regions show the $\pm 1\sigma$ uncertainty. Note that, in this analysis, the PS Tracks dataset used is taken from [15] and cannot be directly compared with the Northern Tracks dataset in the combined sample, which uses track-like events in the northern hemisphere with an updated reconstruction.

The results for the sources close to the center of the Galaxy are given in Fig. 3. The results for this case match the numbers shown in Table. 1, which is expected. One can see that because of the dependence on the IceCube datasets as a function of declination, the PS tracks sample cannot detect any sources (above $N_{Simulated} \sim 3$ for the DP curves) while the other samples can (up to $N_{Simulated} \sim 8$). This is because of the better sensitivity of the DNN and Combined datasets in the Southern Hemisphere.

Next, we show the case for a simulation using a σ_L of 0.01 and 0.5, which simulates the luminosity distribution as a standard candle or log-normal distribution.

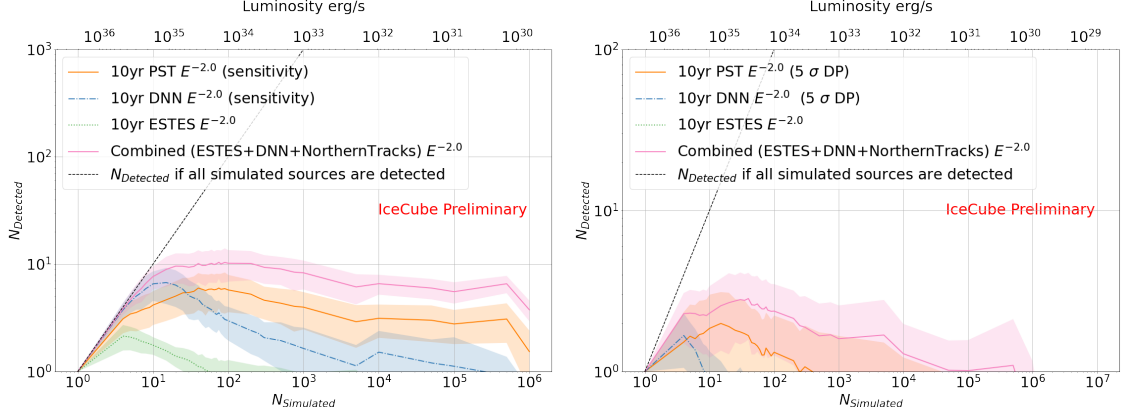


Figure 4: Case for sources simulated with a realistic geometric distribution and a standard candle approach for fluxes: Number of detected neutrino sources using a $\sigma_L=0.01$ and total diffuse flux equals $2.18 \times 10^{-15} \text{ TeV}^{-1} \text{ cm}^{-2} \text{ s}^{-1}$ is compared with different IceCube sensitivity (left) and discovery potential (right) curves, taken from [1, 9, 15]. The 2.18×10^{-15} is obtained using the best-fit neutrino flux derived for the DNN cascade sample using the π^0 template [1] The shaded regions show the 1σ uncertainty.

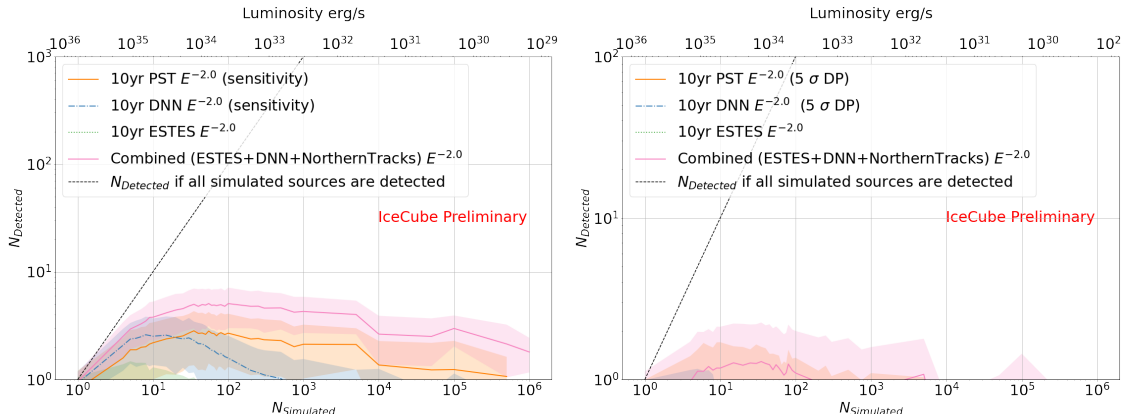


Figure 5: Case for sources simulated with a realistic geometric distribution and a log-normal approach for fluxes: Number of detected neutrino sources using a $\sigma_L=0.5$ and total diffuse flux equals $2.18 \times 10^{-15} \text{ TeV}^{-1} \text{ cm}^{-2} \text{ s}^{-1}$ is compared with different IceCube sensitivity (left) and discovery potential (right) curves, taken from [1, 9, 15]. The shaded regions show the 1σ uncertainty.

Dataset	Quantity	SC ($\sigma_L = 0.01$)	LN ($\sigma_L = 0.5$)	Sources at center
DNN	N_{src}	8	0	6
	L_{mean}	1.4×10^{35}	-	3.5×10^{35}
ESTES	N_{src}	1	0	1
	L_{mean}	2.0×10^{36}	-	2×10^{36}
Combined	N_{src}	1.2×10^5	235	6
	L_{mean}	6.04×10^{30}	1.08×10^{33}	3.5×10^{35}

Table 2: Lower limit on the approximate number of sources (along with the upper limit on the luminosities) detected by each of the datasets based on the simulations. The spectral index used is fixed to 2.0. Note that the results shown in [6] use the 4σ discovery potential curves while this work makes use of the 5σ discovery potential curve for the DNN cascades sample giving a different limit.

4. Angular Resolution (source confusion)

The above simulations estimate the number of detected sources after accounting for Eddington bias and do not take into account the different angular resolutions of the IceCube datasets. As shown in [6], the resolving power of the PS tracks dataset is the best, being able to resolve ~ 26 sources at 100 TeV close to the center, while ESTES and DNN samples are able to resolve ~ 13 and ~ 5 sources respectively. However, because of the improved sensitivity of the DNN sample in the southern hemisphere, sources at the center of the Galaxy are more likely to be detected by DNN cascades. Finally, as the combined sample is a culmination of DNN cascades, ESTES and Northern Tracks, if a source is detected by the combined sample and DNN or ESTES samples, the combined sample will have an equal or better resolving power due to the increased statistics.

5. Discussion

In this work, we simulate Galactic source populations to understand the results presented by [1]. While the ESTES and Combined samples are being used in similar studies (to [1]), we can already use our simulations to explore science cases based on different outcomes of the two studies.

Reference [1] was not able to detect any Galactic sources but detected a neutrino signal from the Galactic Plane. Our simulation shows that if $\lesssim 5$ sources were making up the total neutrino signal, the DNN cascades sample will be able to detect and resolve them. We could extend this calculation to put an upper limit on the number of sources that can be detected by the dataset. This is done by finding the point where the mean number of detected simulated sources, shown in Figs. 3-5, reaches ~ 1 . We report this lower limit in Table. 2 along with calculations using the ESTES and Combined sample datasets.

Our simulation shows that the Combined Sample has the best chance of detecting sources. Based on the combined estimates from Table 1 and 2, we find that the increase in the number of detected sources comes mostly from better sensitivity in the Northern Hemisphere (similar to what

is seen using the PS tracks sample). The simulations using DP curves shown in Figs. 3-5 (right) show that the combined sample outperforms PST in the Northern hemisphere too (seen for larger $N_{Simulated}$ values where flux per source is lower). This is because the combined sample makes use of the Northern Tracks IceCube dataset along with the additional data from DNN and ESTES, which improves the sensitivity. However, we already know that [1] and [15] were not able to detect any sources. Using that fact, if we assume that no sources are detected by the combined sample, we could put a limit of 10^5 SC sources or a limit of ~ 235 sources following a LN distribution. We can also put an upper limit on the luminosity of the source population to be of the order of 10^{33} erg/s. This limit is more constraining because of the improvements in the sensitivity of the combined sample due to the combination of the cascades and tracks datasets, which makes it most sensitive in both the Northern and Southern hemispheres. We can see that from the results depicted here, along with theoretical studies like [5, 6, 17], future improvements and measurements from IceCube are key to understanding exactly how many sources or points of neutrino emission contribute to the Galactic neutrino flux and their nature.

References

- [1] **IceCube** Collaboration, R. Abbasi *et al.* *Science* **380** no. 6652, (2023) 1338–1343.
- [2] T. A. Thompson, A. Burrows, and P. A. Pinto *Astrophys. J.* **592** (2003) 434.
- [3] G. Domokos, B. Elliott, and S. Kovesi-Domokos *Journal of Physics G: Nuclear and Particle Physics* **19** no. 6, (Jun, 1993) 899.
- [4] A. Kheirandish *Astrophys. Space Sci.* **365** no. 6, (2020) 108.
- [5] A. Ambrosone, K. M. Groth, E. Peretti, and M. Ahlers *arXiv e-prints* (June, 2023) .
- [6] A. Desai, J. Vandenbroucke, S. Anandagoda, J. Thwaites, and M. J. Romfoe *arXiv e-prints* (June, 2023) .
- [7] **IceCube** Collaboration, R. Abbasi *et al.* *Nucl. Instrum. Meth. A* **601** (2009) 294–316.
- [8] **IceCube** Collaboration, R. Abbasi *et al.* *PoS ICRC2021* (2021) 1130.
- [9] **IceCube** Collaboration, P. Savina *et al.* *PoS ICRC2023* (these proceedings) 1010.
- [10] **IceCube** Collaboration, R. Abbasi *et al.* *arXiv e-prints* (Jan., 2021) .
- [11] **IceCube** Collaboration, M. Silva and S. Mancina *PoS ICRC2019* (2020) 1010.
- [12] D. Gaggero, D. Grasso, A. Marinelli, A. Urbano, and M. Valli *Astrophys. J. Lett.* **815** no. 2, (2015) L25.
- [13] D. R. Lorimer *et al.* *Mon. Not. Roy. Astron. Soc.* **372** (2006) 777–800.
- [14] M. Ahlers, Y. Bai, V. Barger, and R. Lu *Phys. Rev. D* **93** no. 1, (2016) 013009.
- [15] **IceCube** Collaboration, M. G. Aartsen *et al.* *Phys. Rev. Lett.* **124** no. 5, (2020) 051103.
- [16] N. L. Strotjohann, M. Kowalski, and A. Franckowiak *Astron. Astrophys.* **622** (2019) L9.
- [17] T. Sudoh and J. F. Beacom *Phys. Rev. D* **107** no. 4, (2023) 043002.

Full Author List: IceCube Collaboration

R. Abbasi¹⁷, M. Ackermann⁶³, J. Adams¹⁸, S. K. Agarwalla^{40, 64}, J. A. Aguilar¹², M. Ahlers²², J.M. Alameddine²³, N. M. Amin⁴⁴, K. Andeen⁴², G. Anton²⁶, C. Argüelles¹⁴, Y. Ashida⁵³, S. Athanasiadou⁶³, S. N. Axani⁴⁴, X. Bai⁵⁰, A. Balagopal V.⁴⁰, M. Baricevic⁴⁰, S. W. Barwick³⁰, V. Basu⁴⁰, R. Bay⁸, J. J. Beatty^{20, 21}, J. Becker Tjus^{11, 65}, J. Beise⁶¹, C. Bellenghi²⁷, C. Benning¹, S. BenZvi⁵², D. Berley¹⁹, E. Bernardini⁴⁸, D. Z. Besson³⁶, E. Blaufuss¹⁹, S. Blot⁶³, F. Bontempo³¹, J. Y. Book¹⁴, C. Boscolo Meneguolo⁴⁸, S. Böser⁴¹, O. Botner⁶¹, J. Böttcher¹, E. Bourbeau²², J. Braun⁴⁰, B. Brinson⁶, J. Brostean-Kaiser⁶³, R. T. Burley², R. S. Busse⁴³, D. Butterfield⁴⁰, M. A. Campana⁴⁹, K. Carloni¹⁴, E. G. Carnie-Bronca², S. Chattopadhyay^{40, 64}, N. Chau¹², C. Chen⁶, Z. Chen⁵⁵, D. Chirkin⁴⁰, S. Choi⁵⁶, B. A. Clark¹⁹, L. Classen⁴³, A. Coleman⁶¹, G. H. Collin¹⁵, A. Connolly^{20, 21}, J. M. Conrad¹⁵, P. Coppin¹³, P. Correa¹³, D. F. Cowen^{59, 60}, P. Dave⁶, C. De Clercq¹³, J. J. DeLaunay⁵⁸, D. Delgado¹⁴, S. Deng¹, K. Deoskar⁵⁴, A. Desai⁴⁰, P. Desati⁴⁰, K. D. de Vries¹³, G. de Wasseige³⁷, T. DeYoung²⁴, A. Diaz¹⁵, J. C. Díaz-Vélez⁴⁰, M. Dittmer⁴³, A. Domi²⁶, H. Dujmovic⁴⁰, M. A. DuVernois⁴⁰, T. Ehrhardt⁴¹, P. Eller²⁷, E. Ellinger⁶², S. El Mentawi¹, D. Elsässer²³, R. Engel^{31, 32}, H. Erpenbeck⁴⁰, J. Evans¹⁹, P. A. Evenson⁴⁴, K. L. Fan¹⁹, K. Fang⁴⁰, K. Farrag¹⁶, A. R. Fazzari⁷, A. Fedynitch⁵⁷, N. Feigl¹⁰, S. Fiedlschuster²⁶, C. Finley⁵⁴, L. Fischer⁶³, D. Fox⁵⁹, A. Frankowiak¹¹, A. Fritz⁴¹, P. Fürst¹, J. Gallagher³⁹, E. Ganster¹, A. Garcia¹⁴, L. Gerhardt⁹, A. Ghadimi⁵⁸, C. Glaser⁶¹, T. Glauch²⁷, T. Glüsenskamp^{26, 61}, N. Goehke³², J. G. Gonzalez⁴⁴, S. Goswami⁵⁸, D. Grant²⁴, S. J. Gray¹⁹, O. Gries¹, S. Griffin⁴⁰, S. Griswold⁵², K. M. Groth²², C. Günther¹, P. Gutjahr²³, C. Haack²⁶, A. Hallgren⁶¹, R. Halliday²⁴, L. Halve¹, F. Halzen⁴⁰, H. Hamdaoui⁵⁵, M. Ha Minh²⁷, K. Hanson⁴⁰, J. Hardin¹⁵, A. A. Harnisch²⁴, P. Hatch³³, A. Haungs³¹, K. Helbing⁶², J. Hellrung¹¹, F. Henningsen²⁷, L. Heuermann¹, N. Heyer⁶¹, S. Hickford⁶², A. Hidvegi⁵⁴, C. Hill¹⁶, G. C. Hill², K. D. Hoffman¹⁹, S. Hori⁴⁰, K. Hoshina^{40, 66}, W. Hou³¹, T. Huber³¹, K. Hultqvist²³, M. Hünnefeld²³, R. Hussain⁴⁰, K. Hymon²³, S. In⁵⁶, A. Ishihara¹⁶, M. Jacquart¹⁶, O. Janik¹, M. Jansson⁵⁴, G. S. Japaridze⁵, M. Jeong⁵⁶, M. Jin¹⁴, B. J. P. Jones⁴, D. Kang³¹, W. Kang⁵⁶, X. Kang⁴⁹, A. Kappes⁴³, D. Kappesser⁴¹, L. Kardum²³, T. Karg⁶³, M. Karle²⁷, A. Karle⁴⁰, U. Katz²⁶, M. Kauer⁴⁰, J. L. Kelley⁴⁰, A. Khatee Zathul⁴⁰, A. Kheirandish^{34, 35}, J. Kiryluk⁵⁵, S. R. Klein^{8, 9}, A. Kochocki²⁴, R. Koirala⁴⁴, H. Kolanoski¹⁰, T. Kontrimas²⁷, L. Köpke⁴¹, C. Kopper²⁶, D. J. Koskinen²², P. Koundal³¹, M. Kovacevich⁴⁹, M. Kowalski^{10, 63}, T. Kozynets²², J. Krishnamoorthi^{40, 64}, K. Kruijswijk³⁷, E. Krupczak²⁴, A. Kumar⁶³, E. Kun¹¹, N. Kurahashi⁴⁹, N. Lad⁶³, C. Lagunas Gualda⁶³, M. Lamoureux³⁷, M. J. Larson¹⁹, S. Latseva¹, F. Lauber⁶², J. P. Lazar^{14, 40}, J. W. Lee⁵⁶, K. Leonard DeHolton⁶⁰, A. Leszczyńska⁴⁴, M. Lincetto¹¹, Q. R. Liu⁴⁰, M. Liubarska²⁵, E. Lohfink⁴¹, C. Love⁴⁹, C. J. Lozano Mariscal⁴³, L. Lu⁴⁰, F. Lucarelli²⁸, W. Luszczyk^{20, 21}, Y. Lyu^{8, 9}, J. Madsen⁴⁰, K. B. M. Mahn²⁴, Y. Makino⁴⁰, E. Manao²⁷, S. Mancina^{40, 48}, W. Marie Sainte⁴⁰, I. C. Mariş¹², S. Marka⁴⁶, Z. Marka⁴⁶, M. Marsee⁵⁸, I. Martinez-Soler¹⁴, R. Maruyama⁴⁵, F. Mayhew²⁴, T. McElroy²⁵, F. McNally³⁸, J. V. Mead²², K. Meagher⁴⁰, S. Mechbal⁶³, A. Medina²¹, M. Meier¹⁶, Y. Merckx¹³, L. Merten¹¹, J. Micallef²⁴, J. Mitchell⁷, T. Montaruli²⁸, R. W. Moore²⁵, Y. Morii¹⁶, R. Morse⁴⁰, M. Moulai⁴⁰, T. Mukherjee³¹, R. Naab⁶³, R. Nagai¹⁶, M. Nakos⁴⁰, U. Naumann⁶², J. Necker⁶³, A. Negi⁴, M. Neumann⁴³, H. Niederhausen²⁴, M. U. Nisa²⁴, A. Noell¹, A. Novikov⁴⁴, S. C. Nowicki²⁴, A. Obertacke Pollmann¹⁶, V. O'Dell⁴⁰, M. Oehler³¹, B. Oeyen²⁹, A. Olivas¹⁹, R. Ørsøe²⁷, J. Osborn⁴⁰, E. O'Sullivan⁶¹, H. Pandya⁴⁴, N. Park³³, G. K. Parker⁴, E. N. Paudel⁴⁴, L. Paul^{42, 50}, C. Pérez de los Heros⁶¹, J. Peterson⁴⁰, S. Philippen¹, A. Pizzuto⁴⁰, M. Plum⁵⁰, A. Pontén⁶¹, Y. Popovych⁴¹, M. Prado Rodriguez⁴⁰, B. Pries²⁴, R. Procter-Murphy¹⁹, G. T. Przybylski⁹, C. Raab³⁷, J. Rack-Helleis⁴¹, K. Rawlins³, Z. Rechac⁴⁰, A. Rehman⁴⁴, P. Reichherzer¹¹, G. Renzi¹², E. Resconi²⁷, S. Reusch⁶³, W. Rhode²³, B. Riedel⁴⁰, A. Rifaie¹, E. J. Roberts², S. Robertson^{8, 9}, S. Rodan⁵⁶, G. Roellinghoff⁵⁶, M. Rongen²⁶, C. Rott^{53, 56}, T. Ruhe²³, L. Ruohan²⁷, D. Ryckbosch²⁹, I. Safa^{14, 40}, J. Saffer³², D. Salazar-Gallegos²⁴, P. Sampathkumar³¹, S. E. Sanchez Herrera²⁴, A. Sandrock⁶², M. Santander⁵⁸, S. Sarkar²⁵, S. Sarkar⁴⁷, J. Savelberg¹, P. Savina⁴⁰, M. Schaufel¹, H. Schieler³¹, S. Schindler²⁶, L. Schlickmann¹, B. Schlüter⁴³, F. Schlüter¹², N. Schmeisser⁶², T. Schmidt¹⁹, J. Schneider²⁶, F. G. Schröder^{31, 44}, L. Schumacher²⁶, G. Schwefer¹, S. Sclafani¹⁹, D. Seckel⁴⁴, M. Seikh³⁶, S. Seunarine⁵¹, R. Shah⁴⁹, A. Sharma⁶¹, S. Shefali³², N. Shimizu¹⁶, M. Silva⁴⁰, B. Skrzypek¹⁴, B. Smithers⁴, R. Snihur⁴⁰, J. Soedingrekso²³, A. Sogaard²², D. Soldin³², P. Soldin¹, G. Sommani¹¹, C. Spannfellner²⁷, G. M. Spiczak⁵¹, C. Spiering⁶³, M. Stamatikos²¹, T. Stanev⁴⁴, T. Stetzelberger⁹, T. Stürwald⁶², T. Stuttard²², G. W. Sullivan¹⁹, I. Taboada⁶, S. Ter-Antonyan⁷, M. Thiesmeyer¹, W. G. Thompson¹⁴, J. Thwaites⁴⁰, S. Tilav⁴⁴, K. Tollefson²⁴, C. Tönnes⁵⁶, S. Toscano¹², D. Tosi⁴⁰, A. Trettin⁶³, C. F. Tung⁶, R. Turcotte³¹, J. P. Twagirayezu²⁴, B. Ty⁴⁰, M. A. Unland Elorrieta⁴³, A. K. Upadhyay^{40, 64}, K. Upshaw⁷, N. Valtonen-Mattila⁶¹, J. Vandenbroucke⁴⁰, N. van Eijndhoven¹³, D. Vannerom¹⁵, J. van Santen⁶³, J. Vara⁴³, J. Veitch-Michaelis⁴⁰, M. Venugopal³¹, M. Vereecken³⁷, S. Verpoest⁴⁴, D. Veske⁴⁶, A. Vijai¹⁹, C. Walck⁵⁴, C. Weaver²⁴, P. Weigel¹⁵, A. Weindl³¹, J. Weldert⁶⁰, C. Wendt⁴⁰, J. Werthebach²³, M. Weyrauch³¹, N. Whitehorn²⁴, C. H. Wiebusch¹, N. Willey²⁴, D. R. Williams⁵⁸, L. Witthaus²³, A. Wolf¹, M. Wolf²⁷, G. Wrede²⁶, X. W. Xu⁷, J. P. Yanez²⁵, E. Yildizci⁴⁰, S. Yoshida¹⁶, R. Young³⁶, F. Yu¹⁴, S. Yu²⁴, T. Yuan⁴⁰, Z. Zhang⁵⁵, P. Zhelnin¹⁴, M. Zimmerman⁴⁰

¹ III. Physikalisches Institut, RWTH Aachen University, D-52056 Aachen, Germany

² Department of Physics, University of Adelaide, Adelaide, 5005, Australia

³ Dept. of Physics and Astronomy, University of Alaska Anchorage, 3211 Providence Dr., Anchorage, AK 99508, USA

⁴ Dept. of Physics, University of Texas at Arlington, 502 Yates St., Science Hall Rm 108, Box 19059, Arlington, TX 76019, USA

⁵ CTSPS, Clark-Atlanta University, Atlanta, GA 30314, USA

⁶ School of Physics and Center for Relativistic Astrophysics, Georgia Institute of Technology, Atlanta, GA 30332, USA

⁷ Dept. of Physics, Southern University, Baton Rouge, LA 70813, USA

⁸ Dept. of Physics, University of California, Berkeley, CA 94720, USA

⁹ Lawrence Berkeley National Laboratory, Berkeley, CA 94720, USA

¹⁰ Institut für Physik, Humboldt-Universität zu Berlin, D-12489 Berlin, Germany

¹¹ Fakultät für Physik & Astronomie, Ruhr-Universität Bochum, D-44780 Bochum, Germany

¹² Université Libre de Bruxelles, Science Faculty CP230, B-1050 Brussels, Belgium

- ¹³ Vrije Universiteit Brussel (VUB), Dienst ELEM, B-1050 Brussels, Belgium
¹⁴ Department of Physics and Laboratory for Particle Physics and Cosmology, Harvard University, Cambridge, MA 02138, USA
¹⁵ Dept. of Physics, Massachusetts Institute of Technology, Cambridge, MA 02139, USA
¹⁶ Dept. of Physics and The International Center for Hadron Astrophysics, Chiba University, Chiba 263-8522, Japan
¹⁷ Department of Physics, Loyola University Chicago, Chicago, IL 60660, USA
¹⁸ Dept. of Physics and Astronomy, University of Canterbury, Private Bag 4800, Christchurch, New Zealand
¹⁹ Dept. of Physics, University of Maryland, College Park, MD 20742, USA
²⁰ Dept. of Astronomy, Ohio State University, Columbus, OH 43210, USA
²¹ Dept. of Physics and Center for Cosmology and Astro-Particle Physics, Ohio State University, Columbus, OH 43210, USA
²² Niels Bohr Institute, University of Copenhagen, DK-2100 Copenhagen, Denmark
²³ Dept. of Physics, TU Dortmund University, D-44221 Dortmund, Germany
²⁴ Dept. of Physics and Astronomy, Michigan State University, East Lansing, MI 48824, USA
²⁵ Dept. of Physics, University of Alberta, Edmonton, Alberta, Canada T6G 2E1
²⁶ Erlangen Centre for Astroparticle Physics, Friedrich-Alexander-Universität Erlangen-Nürnberg, D-91058 Erlangen, Germany
²⁷ Technical University of Munich, TUM School of Natural Sciences, Department of Physics, D-85748 Garching bei München, Germany
²⁸ Département de physique nucléaire et corpusculaire, Université de Genève, CH-1211 Genève, Switzerland
²⁹ Dept. of Physics and Astronomy, University of Gent, B-9000 Gent, Belgium
³⁰ Dept. of Physics and Astronomy, University of California, Irvine, CA 92697, USA
³¹ Karlsruhe Institute of Technology, Institute for Astroparticle Physics, D-76021 Karlsruhe, Germany
³² Karlsruhe Institute of Technology, Institute of Experimental Particle Physics, D-76021 Karlsruhe, Germany
³³ Dept. of Physics, Engineering Physics, and Astronomy, Queen's University, Kingston, ON K7L 3N6, Canada
³⁴ Department of Physics & Astronomy, University of Nevada, Las Vegas, NV, 89154, USA
³⁵ Nevada Center for Astrophysics, University of Nevada, Las Vegas, NV 89154, USA
³⁶ Dept. of Physics and Astronomy, University of Kansas, Lawrence, KS 66045, USA
³⁷ Centre for Cosmology, Particle Physics and Phenomenology - CP3, Université catholique de Louvain, Louvain-la-Neuve, Belgium
³⁸ Department of Physics, Mercer University, Macon, GA 31207-0001, USA
³⁹ Dept. of Astronomy, University of Wisconsin–Madison, Madison, WI 53706, USA
⁴⁰ Dept. of Physics and Wisconsin IceCube Particle Astrophysics Center, University of Wisconsin–Madison, Madison, WI 53706, USA
⁴¹ Institute of Physics, University of Mainz, Staudinger Weg 7, D-55099 Mainz, Germany
⁴² Department of Physics, Marquette University, Milwaukee, WI, 53201, USA
⁴³ Institut für Kernphysik, Westfälische Wilhelms-Universität Münster, D-48149 Münster, Germany
⁴⁴ Bartol Research Institute and Dept. of Physics and Astronomy, University of Delaware, Newark, DE 19716, USA
⁴⁵ Dept. of Physics, Yale University, New Haven, CT 06520, USA
⁴⁶ Columbia Astrophysics and Nevis Laboratories, Columbia University, New York, NY 10027, USA
⁴⁷ Dept. of Physics, University of Oxford, Parks Road, Oxford OX1 3PU, United Kingdom
⁴⁸ Dipartimento di Fisica e Astronomia Galileo Galilei, Università Degli Studi di Padova, 35122 Padova PD, Italy
⁴⁹ Dept. of Physics, Drexel University, 3141 Chestnut Street, Philadelphia, PA 19104, USA
⁵⁰ Physics Department, South Dakota School of Mines and Technology, Rapid City, SD 57701, USA
⁵¹ Dept. of Physics, University of Wisconsin, River Falls, WI 54022, USA
⁵² Dept. of Physics and Astronomy, University of Rochester, Rochester, NY 14627, USA
⁵³ Department of Physics and Astronomy, University of Utah, Salt Lake City, UT 84112, USA
⁵⁴ Oskar Klein Centre and Dept. of Physics, Stockholm University, SE-10691 Stockholm, Sweden
⁵⁵ Dept. of Physics and Astronomy, Stony Brook University, Stony Brook, NY 11794-3800, USA
⁵⁶ Dept. of Physics, Sungkyunkwan University, Suwon 16419, Korea
⁵⁷ Institute of Physics, Academia Sinica, Taipei, 11529, Taiwan
⁵⁸ Dept. of Physics and Astronomy, University of Alabama, Tuscaloosa, AL 35487, USA
⁵⁹ Dept. of Astronomy and Astrophysics, Pennsylvania State University, University Park, PA 16802, USA
⁶⁰ Dept. of Physics, Pennsylvania State University, University Park, PA 16802, USA
⁶¹ Dept. of Physics and Astronomy, Uppsala University, Box 516, S-75120 Uppsala, Sweden
⁶² Dept. of Physics, University of Wuppertal, D-42119 Wuppertal, Germany
⁶³ Deutsches Elektronen-Synchrotron DESY, Platanenallee 6, 15738 Zeuthen, Germany
⁶⁴ Institute of Physics, Sachivalaya Marg, Sainik School Post, Bhubaneswar 751005, India
⁶⁵ Department of Space, Earth and Environment, Chalmers University of Technology, 412 96 Gothenburg, Sweden
⁶⁶ Earthquake Research Institute, University of Tokyo, Bunkyo, Tokyo 113-0032, Japan

Acknowledgements

The authors gratefully acknowledge the support from the following agencies and institutions: USA – U.S. National Science Foundation-Office of Polar Programs, U.S. National Science Foundation-Physics Division, U.S. National Science Foundation-EPSCoR, Wisconsin Alumni Research Foundation, Center for High Throughput Computing (CHTC) at the University of Wisconsin–Madison, Open Science

Grid (OSG), Advanced Cyberinfrastructure Coordination Ecosystem: Services & Support (ACCESS), Frontera computing project at the Texas Advanced Computing Center, U.S. Department of Energy-National Energy Research Scientific Computing Center, Particle astrophysics research computing center at the University of Maryland, Institute for Cyber-Enabled Research at Michigan State University, and Astroparticle physics computational facility at Marquette University; Belgium – Funds for Scientific Research (FRS-FNRS and FWO), FWO Odysseus and Big Science programmes, and Belgian Federal Science Policy Office (Belspo); Germany – Bundesministerium für Bildung und Forschung (BMBF), Deutsche Forschungsgemeinschaft (DFG), Helmholtz Alliance for Astroparticle Physics (HAP), Initiative and Networking Fund of the Helmholtz Association, Deutsches Elektronen Synchrotron (DESY), and High Performance Computing cluster of the RWTH Aachen; Sweden – Swedish Research Council, Swedish Polar Research Secretariat, Swedish National Infrastructure for Computing (SNIC), and Knut and Alice Wallenberg Foundation; European Union – EGI Advanced Computing for research; Australia – Australian Research Council; Canada – Natural Sciences and Engineering Research Council of Canada, Calcul Québec, Compute Ontario, Canada Foundation for Innovation, WestGrid, and Compute Canada; Denmark – Villum Fonden, Carlsberg Foundation, and European Commission; New Zealand – Marsden Fund; Japan – Japan Society for Promotion of Science (JSPS) and Institute for Global Prominent Research (IGPR) of Chiba University; Korea – National Research Foundation of Korea (NRF); Switzerland – Swiss National Science Foundation (SNSF); United Kingdom – Department of Physics, University of Oxford.